Research and Reviews: Journal of Pharmacy and Pharmaceutical Sciences

Chemicobiological Deciphering the Protein-Binding Details of Aspirin

Hang-Xing Xiong, Hong-Lin Wang, Hua-Xin Zhang and Li-Wei Li*

College of Chemical and Pharmaceutical Engineering, Jingchu University of Technology,
Jingmen, Hubei 448000, People's Republic of China

Research Article

*For Correspondence

Li-wei Li, College of Chemical and Pharmaceutical Engineering, Jingchu University of Technology, Jingmen, Hubei 448000, People's Republic of China, Tel: 86-724-2355811

E-mail: jmlilwei1005@163.com

ABSTRACT

Fluorescence quenching and fluorescence resonance energy transfer (FRET) theories are widely used in drug-protein binding study, but the inner filter effect is not always being corrected, which may cause inaccurate results. In view of this, the interaction of aspirin (ASP) with human serum albumin (HSA) was studied by three-dimensional fluorescence spectra, ultraviolet spectra, circular dichroism (CD) spectra, and molecular modeling methods. The inner effect was subtracted from raw data of the fluorescence when evaluating the number of binding sites, equilibrium constants, and thermodynamic parameters. The results showed that only one binding site formed on HSA and it obviously impaired by increasing temperature. The negative Gibbs free energy change (G^θ) suggested the binding was spontaneous. Meanwhile, negative enthalpy change (H^θ) and entropy change (S^θ) indicated hydrogen bonds had an important influence in the formation of ASP-HSA complex. The distance between donor and acceptor was calculated according to Förster's non-radiation resonance energy transfer theory using the corrected fluorescence data. Synchronous spectra implied the polarity of tryptophan residue increased, which gave a clue to binding location. CD spectra were employed to detect the secondary structural changes of HSA. Based on experimental results, molecular modeling was carried out to calculate the most optimized docking mode, in which both panorama and details were involved.

INTRODUCTION

One of significant factors to be considered on the pharmaceutical action of drugs is their binding tendency to plasma proteins [1]. The extent of protein binding in the plasma or tissue controls the volume of distribution and affects both hepatic and renal clearance [1,2]. Human serum albumin (HSA), generally regarded as a nonspecific transport protein, is a monomeric multi-domain macromolecule, representing the main determinant of plasma oncotic pressure and the main modulator of fluid distribution between body compartments [3], being primarily protein model in drug-protein binding research [4]. Aspirin, also known as acetylsalicylic acid (ASP; formula: $C_9H_8O_4$; CAS Registry number: 50-78-2), is a salicylate drug, clinically used in the treatment of a wide range of conditions, including fever, pain, rheumatic fever, and inflammatory diseases, such as rheumatoid arthritis, pericarditis [5]. ASP also has an antiplatelet effect by inhibiting the production of thromboxane, which under normal circumstances binds platelet molecules together to create a patch over damaged walls of blood vessels and the platelet patch can become large enough to block blood flow, locally and downstream [6]. Lower doses of ASP have also shown to reduce the risk of death from a heart attack or the risk of stroke in some circumstances [7]. There is some evidence that ASP is effective at preventing colorectal cancer, particularly colorectal cancer, though the mechanisms of this effect are unclear [5,8].

For such an important drug, it's not surprising to find documents regarding to its interaction with serum albumins [9,10]. Binding equilibrium and binding geometry were involved in some references employing fluorescence method [11-13], but the inner

filter effects were not corrected in calculation, which might impair the accuracy of partial results [14,15]. In addition, previous work did not give the thermodynamics of the interaction, which made it difficult to evaluate the nature of binding forces.

The purpose of this work was to investigate the binding reaction of ASP to HSA under simulated physiological conditions (ionic strength=0.1 mol·L^{-1}; pH 7.40; aqueous solution) by multiple spectroscopic methods, to calculate binding constant, the number of binding sites and binding location using the data that have subtracted inner filter effects, to analyze the nature of binding forces from thermodynamic parameters, to detect structural changes of HSA, and to model the molecule structure of new complex according to experimental data.

EXPERIMENTAL

Materials

HSA was purchased from Sigma (USA, 99%). ASP, Tris, HCl, NaCl were purchased from Shanghai Chemical Reagent Company (China). All other chemicals were of analytical grade. Stock solutions of HSA (10^{-5} mol·L^{-1}), ASP (10^{-3} mol·L^{-1}), NaCl (0.5 mol·L^{-1}) and Tris-HCl buffer (0.05 mol·L^{-1} Tris, 0.15 mol·L^{-1} HCl) of pH 7.40 were prepared by directly dissolving the original reagents. Water used to prepare solutions was double-distilled.

Instrumental Methods

All fluorescence spectra were recorded on F-4600 Fluorescence Spectrofluorimetry (Hitachi, Japan) equipped with 1.0 cm quartz cells and a thermostat bath. To obtain smooth emission spectra with moderate intensity, the widths of excitation slit and emission slit were both set at 5 nm. The scanning speed was set at 2400 nm per minute. An excitation wavelength of 275nm was chosen and appropriate blanks corresponding to the buffer were subtracted to correct the background. UV spectra were recorded at different temperature on a TU-1901 spectrophotometer (Purkinje General, China) equipped with 1.0 cm quartz cells. Circular dichroism (CD) measurements were performed at 311 K on a J-810 Spectro-polarimeter (Jasco, Japan) equipped with 1.0 cm quartz cells over a wavelength range of 260-200 nm and under constant nitrogen flush at a scanning speed of 200 nm per min. The pH measurements were made with a pHS-3 digital pH-meter (Shanghai, China). All weight measurements were performed with an AY-120 electronic analytic weighing scale (Shimadzu, Japan).

Inner Filter Effect

Inner-filter effect refers to the absorption of radiation going towards (excitation) or emanating from (emission). The fluorophore and it is important to subtract such an effect from the raw data of the fluorescence [14]. To correct the inner filter effects of HSA and ASP, absorbance was measured at excitation and emission wavelengths. The fluorescence intensity was corrected using the equation (1):

$$F_{cor} = F_{obs} 10^{\frac{1}{2}(Aex+Aem)} \tag{1}$$

Where F_{cor} and F_{obs} are the fluorescence intensities corrected and observed, respectively, and A_{ex} and A_{em} are the absorption of the systems at the excitation and the emission wavelength, respectively. All the fluorescence intensity used in this paper is corrected intensity, with an exception of three-dimensional fluorescence spectra.

Molecular Modeling

Molecular modeling calculations were carried out using Sybyl 8.1. The crystal structure of HSA was from Brookhaven proteins data bank (PDB) database (entry codes: 1h9z for site I, 2bxg for site II). All the ligands and water molecules were removed before the analysis. H atoms were added and the biopolymer was charged using AMBER7 FF99 method. The site of the protein was defined with ligand (A/WRR2001 for site I, A/IBP2001 for site II); the principal regions of ligand binding to HSA were analyzed with Sybyl 8.1 software. The structure of ASP was generated with sybyl 8.1 package and the molecule was optimized (energy minimization) using Tripos Force Field after being charged with Gasteiger and Marsili method. The docking mode of ASP with HSA was conducted by a Surflex-Dock program in Sybyl 8.1 package.

RESULTS AND DISCUSSIONS

Three-dimensional Fluorescence Spectra

Fluorescence allows a non-destructive way of tracking or analysis of biological molecules [16,17] and has been widely used in life science as it occurs in nature in various biological systems [17,18]. Fluorescence is a function of the excitation wavelength and emission wavelength, so full fluorescence information of a phosphor can only be descript by three-dimensional (3D) fluorescence spectrum, in which a stereopsis containing excitation wavelength, emission wavelength and fluorescence intensity is recorded. According to experimental procedures, 3D fluorescence spectra of HSA in the absence and in the presence of ASP were recorded and shown in **Figure 1** The information of fluorescence peaks was listed in **Table 1.**
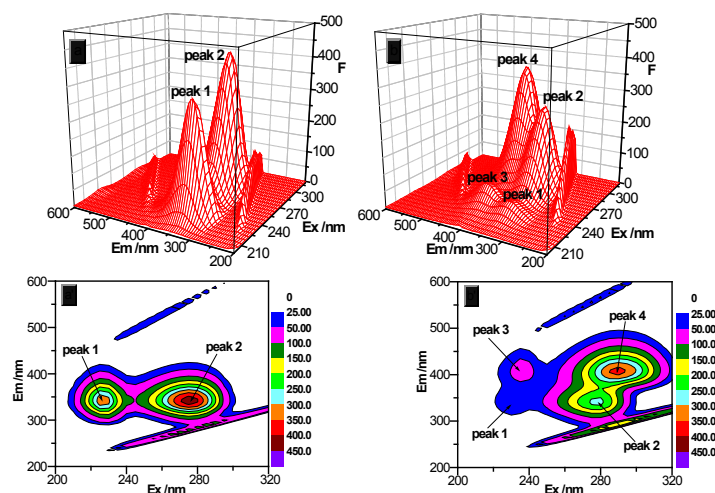
Figure 1. Three-dimensional fluorescence spectra of HSA (a, a') and HSA-ASP (b, b') systems (cHSA= 2.0 × 10⁻⁶ mol L⁻¹, cAZN= 3.5 × 10⁻⁴ mol L⁻¹; a' and b' are the contour of a and b, respectively).

Table 1. Characteristic parameters of three-dimensional fluorescence peaks.

Systems and parameters		Peak 1	Peak 2
HSA	Peak position ($\lambda ex/\lambda em$, nm/nm)	225.0/340.0	275.0/340.0
	Relative intensity	334.8	425.6
	Stokes shift $\Delta \lambda$/nm	115	65
HSA-ASP	Peak position ($\lambda ex/\lambda em$, nm/nm)	230.0/340.0	280.0/340.0
	Relative intensity	45.50	262.6
	Stokes shift $\Delta\lambda$/nm	110	60

Two typical fluorescence peaks of HSA in **Figure 1** were labeled as peak1 and peak 2, respectively. Peak 3 (235.0/340.0, 71.54) and peak 4 (290.0/410.0, 366.1) were typical fluorescence peaks of ASP. The intensity of peak 2 is obviously higher than peak 1, so the excitation frequency of peak 2 (275 nm) was selected as the best excitation wavelength in following experiments. The intensity of these two peaks significantly decreased when ASP was added, which is commonly known as fluorescence quenching.

UV Absorption Spectra

Fluorescence quenching can be caused by a lot of physical and chemical processes [19], but can be classified as either dynamic or static mechanism [20]. Static mechanism refers to radiation decrease caused by ground-state complex formation, in which process the absorption of phosphor and quencher always alters as the absorption spectra of HSA are sensitive to the microenvironment surrounding the chromophore [21]. **Figure 2** displays the UV absorption spectra of HSA, ASP, HSA-ASP systems. In **Figure 2,** curve b' is the physical superposition of absorbance of HSA and ASP. It is obviously different from the spectrum of HSA-ASP system (curve b), which gives a hint that new compound formed. As shown in **Figure 2,** HSA has an absorption peak at 275 nm, which coincides with the typical fluorescence peak of HSA in 3D spectra. Meanwhile, ASP can also absorb the radiation at 275 nm, which means its inner filter effect cannot be ignored [22].
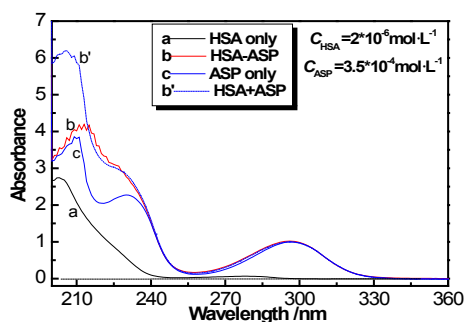
**Figure 2.** UV absorption spectra of HSA, ASP and HSA-ASP systems.

Quenching Mechanism Analysis

In order to ascertain the quenching mechanism, the emission spectra of HSA in the presence of different Amount of ASP were

recorded when the excitation wavelength was stabilized at 275 nm, as shown in **Figure 3.** Supposing the quenching was dynamic quenching, the fluorescence data at different temperatures could be analyzed with the well-known Stern-Volmer equation [23,24]:

$$\frac{F_0}{F} = 1 + K_{SV}[Q] = 1 + K_q \tau_0 [Q] \tag{2}$$

Where F_0 and F are the fluorescence intensity in absence and in presence of quencher, respectively, K_{SV} is the Stern-Volmer quenching constant, [Q] is the concentration of the quencher. K_q the quenching rate constant of the biological macromolecule and $K_q = K_{SV}/\tau_0$, τ_0 is the life time of the fluorophore in the absence of quencher and the life time of the biopolymer is equal to 10^{-8} s [25]. Equation 2 could be applied to determine K_{SV} by linear regression of a plot of F_0/F against [Q]. **Figure 4** displayed the Stern-Volmer plots of the fluorescence quenching of HSA by ASP at four different temperatures, the corresponding K_{SV} at each temperature were calculated and listed in **Table 2.**
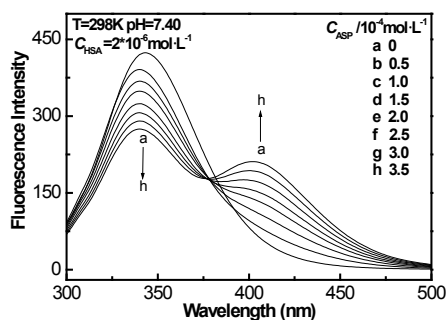
Figure 3. Fluorescence emission spectra of HSA-ASP systems.

Dynamic quenching is caused by collision [26,27], the maximum scatter collision quenching constant of various quenchers with biopolymer is 2.0×10^{10} L·mol^{-1}·s^{-1} [28], but it is obvious that the rate constants K_q shown in **Table 2** are greater than 2.0×10^{10} L·mol^{-1}·s^{-1}. These results indicate that the quenching was not initiated from dynamic collision but from the formation of a new complex [21].
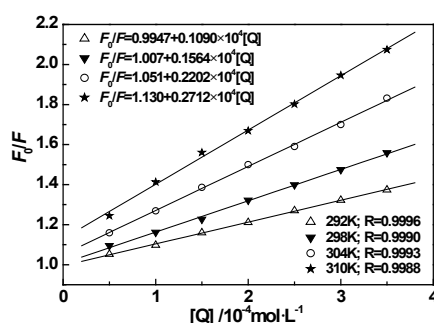
Figure 4. Stern-Volmer plots for the quenching of HSA by ASP.

Table 2. Stern-Volmer constants.

pH	T(K)	K_{SV} (10^{3}L·mol^{-1})	K_q (10^{11}L·mol^{-1}·s^{-1})	SD*
7.4	292	1.096	1.096	0.0037
	298	1.554	1.554	0.0082
	304	2.096	2.096	0.0096
	310	2.400	2.400	0.016

*SD is the standard deviation for K_{SV}

Binding Equilibrium and Thermodynamics

About 50-80% of ASP in the blood is bound to albumin protein, while the rest remains in the active, ionized

state. For a static quenching process, the binding equilibrium can be determined by following equation 3 [15,29]:

$$\log\left(\frac{F_0 - F}{F}\right) = \log K_b + n \log[Q] \tag{3}$$

Where F_0, F, and [Q] are the same as in eq 2, K_b is observed binding constant and n is the number of binding sites per HSA molecule. The value of log ($F_0/F-1$) is linear with the value of log [Q], in which the slope is the number of binding site (n) whereas the intercept (ordinate at the origin) is the logarithm value of K_b (log K_b). The regression curves and equations were shown in **Figure 5.** The corresponding K_b and the number of binding sites (n) were calculated and list in **Table 3.** The value of observed binding constant decreased with the increasing temperature, which indicated the stability of new complex was strikingly affected by temperature.
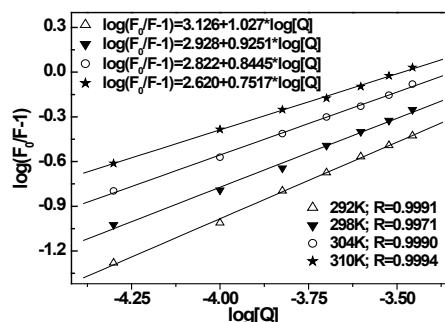
Figure 5. Log (F0/F−1)-log [Q] plots at different temperatures.

In order to estimate the type of affinity between ASP and HSA, the enthalpy change and entropy change of the interaction are important [30,31]. Therefore, the dependence of binding constant on temperature was studied using the equation (4,5):

$$\ln K = \frac{-\Delta H^{\theta}}{RT} + \frac{\Delta S^{\theta}}{R}$$ (4)

$$\Delta G^{\theta} = \Delta H^{\theta} - T \cdot \Delta S^{\theta}$$ (5)

Where H^{θ}, G^{θ} and S^{θ} are enthalpy change, Gibbs free energy change and entropy change, respectively. The plot of log$K$ versus $1/T$ (Van't Hoff plot) enables the determination of H^{θ}, S^{θ} in isobaric processes and G^{θ} can be calculated by eq. (5). Van't Hoff plot was shown in **Figure 6** and thermodynamic parameters were listed in **Table 3.** The negative G^{θ} in **Table 3** indicated the interaction between ASP and HSA was spontaneous under physiological conditions. The negative H^{θ} suggested the binding reaction was an exothermic process, which could in turn give reasonable explanations for the decreasing value of K_b and n with temperature in **Table 3.** The negative S^{θ} suggested the interaction was entropy-driven.

Based on the views of Ross and Subramanian [32], positive S^{θ} value represents the existence of hydrophobic interaction. Negative S^{θ} and H^{θ} always reflects van der Waals force or hydrogen bond formation. $H^{\theta} \approx 0$ may be a clue of electrostatic force. Based on these rules, it can be speculated that hydrogen bond and van der Waals power were the major contributors in stabilizing the structure of HSA-ASP complex.
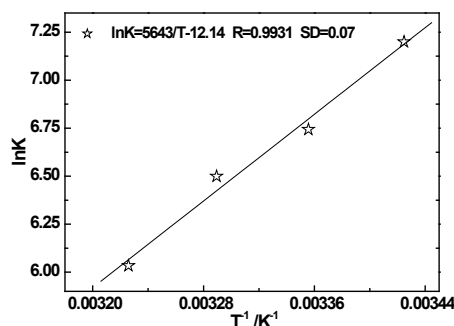

Figure 6. Van't Hoff plot for the binding of ASP with HAS.

Table 3. Observed binding constants, binding sites and thermodynamic parameters.

pH	T(K)	K_b(L·mol^{-1})	n	SD[a]	ΔH$^{\theta}$ (kJ·mol^{-1})	ΔS$^{\theta}$ (J·K^{-1})	ΔG$^{\theta}$ (kJ·mol^{-1})
7.40	293	$10^{3.126}$	1.027	0.014	-46.92	-100.9	-17.45
	299	$10^{2.928}$	0.9251	0.023			-16.84
	305	$10^{2.822}$	0.8445	0.012			-16.24
	311	$10^{2.620}$	0.7517	0.009			-15.63
[a]SD is the standard deviation for K_b							

Conformation Investigation

Synchronous fluorescence spectra can give the characteristic information of tryptophan residues and tyrosine residues when the wavelength shift (Δλ) between excitation and emission wavelength was stabilized at 60 nm and 15nm, respectively [25]. As shown in **Figure 7**, a red shift could be observed on the synchronous fluorescence spectra of tryptophan residues (Δλ=60 nm), which indicated the environmental polarity around tryptophan residues increased because of the binding of ASP [24,33].

To confirm the concrete influence of ASP binding on the secondary structure of HSA, circular dichroism (CD) spectroscopy is used, which has been used to examine proteins, polypeptides, and peptide structures. CD spectrum in the far ultraviolet (UV) regions are dominated by the $n{\to}\pi^*$ and $\pi{\to}\pi^*$ transitions of amide groups, and are influenced by the geometries of the polypeptide backbones [34,35]. CD spectrum of HSA exhibits two negative bands at 208 and 222 nm which reflect the characteristic

of α-helix in the advanced structure of protein as these two negative peaks are both contributed to $n{\rightarrow}\pi^*$ transfer for the peptide bond of α-helical [34]. CD results can be expressed in terms of mean residue elasticity (MRE) in deg cm^2 d mol^{-1} according to the following Equation 6:

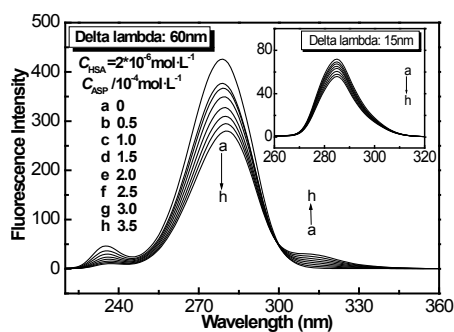**Figure 7.** Synchronous fluorescence spectra of HSA system.

$$MRE = \frac{Observed\ \mathrm{CD}(m\mathrm{deg})}{C_{\mathrm{p}}nl \times 10} \tag{6}$$

Where C_{p} is the molar concentration of the protein, n the number of amino acid residues and l is the path length (0.1cm). The α-helical contents of free and combined HSA were calculated from MRE values at 208 nm using the (equation 7) [36,37].

$$\alpha\text{-}helix\ (\%) = \frac{-MRE_{208} - 4000}{33000 - 4000} \tag{7}$$

Where MRE_{208} is the observed MRE value at 208 nm, 4000 is the MRE of the β-form and random coil conformation cross at 208 nm and 33,000 is the MRE value of a pure α-helix at 208 nm.

CD measurements in absence of and in presence of ASP were performed **(Figure 8).** The estimations for secondary structural elements using SELCON3 software are listed in **Table 4.** A reduction of the α-helix from 59.8% (free HSA) to 54.6% was detected at concentration ratio of 10:1for ASP: HSA. This could be explained by the changes of hydrogen bonding networks on the main polypeptide chain of HSA, which resulted from ASP's binding to the amino acid residues by new hydrogen bonds [38]. In addition to this, more detailed secondary structure changes including regular α-helix, distorted α-helix, regular β-strand, distorted β-strand, β-turns and unordered structure, were also involved in **Table 4.**
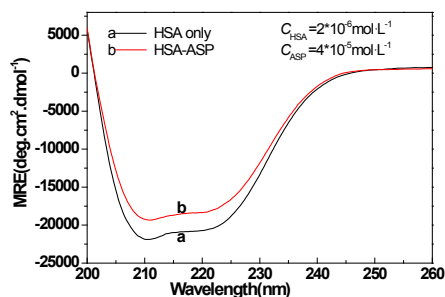

Figure 8. The CD spectrum of HSA and ASP-HSA system.

Table 4. Fractions of different secondary structures determined by SELCON3[a].

System	H(r) (%)	H(d) (%)	S(r) (%)	S(d) (%)	Trn (%)	Unrd (%)
HSA	40.2	19.6	2.9	3.0	12.9	20.8
HSA-ASP	35.1	19.5	4.4	4.5	16.4	23.2

[a] H(r): regular α-helix; H (d): distorted α-helix; S(r): regular β-strand; S(d): distorted β-strand; Trn: β-turns; Unrd: unordered structure.

Energy Transfer between ASP and HAS

According to Forester's non-radioactive fluorescence resonance energy transfer theory [39], energy transfer can take place through direct electrodynamics interaction when (i) The donor can produce fluorescence light; (ii) fluorescence emission spectrum of the donor and UV–vis absorbance spectrum of the acceptor have more overlap; and (iii) the distance between the donor and the acceptor is no longer than 8 nm [40]. In detail, it can be described by the following (equations 8-10) [33,41,42].

$$E = \frac{R_0^6}{R_0^6 + r^6} = 1 - \frac{F}{F_0} \tag{8}$$

$$R_0 = 0.211(K^2\phi\ N^{-4}J)^{1/6} \tag{9}$$

$$J = \frac{\int_0^\infty F_D(\lambda)\varepsilon_A(\lambda_0)\lambda^4 d\lambda}{\int_0^\infty F_D(\lambda)d\lambda} \tag{10}$$

where E is the efficiency of transfer between the donor and the acceptor, R_0 the critical distance when the efficiency of transfer 50%, r the distance between the acceptor and the donor, K^2 the space factor of orientation, N the refractive index of medium, ϕ the fluorescence quantum yield of the donor, J the effect of the spectral overlap between the emission spectrum of the donor and the absorption spectrum of the acceptor, $F_D(\lambda)$ the corrected fluorescence intensity of the donor in the wavelength range λ_0 to λ, and $\varepsilon_A(\lambda_0)$ the extinction coefficient of the acceptor at λ_0.

The overlap of the absorption spectrum of ASP and the fluorescence emission spectrum of HSA is shown in **Figure 9.** The overlap integral, J, can be evaluated by integrating the spectra in **Figure 9** according to the Equation (10). Under present experimental conditions, $K^2=2/3$, $N=1.336$ and $\phi=0.118$ could be used [17]. Finally, the values of these parameters were found to be: $J=1.976\times10^{13}$ L mol^{-1} cm^{-1} nm^4, $R_0=1.87$ nm, $E=0.016$ and $r=3.71$ nm. So the distance between the ASP and the donor (tryptophan in HSA) was 3.71 nm.
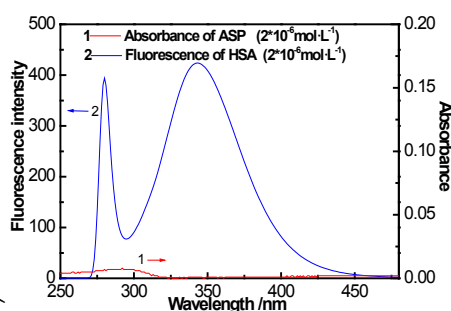

Figure 9. Absorption spectrum of ASP and fluorescence emission spectrum of HSA.

Molecular Modeling

Crystallographic analyses revealed there are in HSA' structure 585 amino acid residues which are divided into three homologous a-helical domains, named as domain I (residues 1-195), domain II (residues 196-383) and domain III (residues 384-585) [43,44]. Each domain contains 10 helices that is divided into antiparallel six-helix and four-helix subdomains, marked by A and B, respectively [4,45]. Aromatic and heterocyclic ligands were found to bind within two hydrophobic pockets in subdomains IIA and IIIA [46]. In **Table 3**, the number of binding sites n was closed to 1, which indicated HSA molecule had only one binding site for ASP under specified conditions. Previous studies [11] proved that ASP bond in the subdomain IIA of HSA, which is also named Sudlow's site I according to Sudlow's nomenclature [47]. This is also supported by energy transfer calculation because there is in HSA the only one tryptophan residue locating in the subdomain IIA [43,48].

In order to visually present the binding mode of ASP to HSA, molecular modeling method was employed. In our work, Sybyl 8.1 software was selected to evaluate the most reasonable mode of the interactions. The highest scoring binding site was. To further unfold the binding details, molecule docking was performed by Suflex-dock program in Sybyl 8.1 and the best energy ranked result was enlarged and displayed in **Figure 10,** where the residues adjacent to ASP were presented by lines.
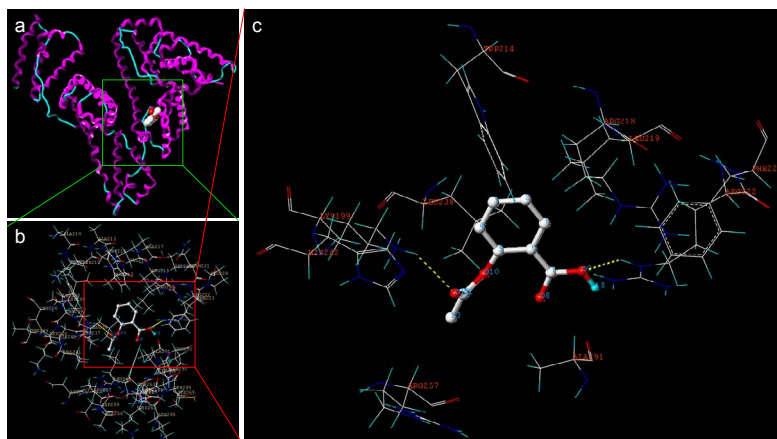
Figure 10. Molecular modeling of interaction between ASP and HSA.

It was evident that ASP molecule lay within subdomain IIA, adjacent to several hydrophobic amino acid residues including LEU219, LEU238, TRP214, ALA291 and PHE223. This indicated that hydrophobic forces had contributed to the interaction [49]. In addition, there were hydrogen bonds between ASP and residues of HSA marked by yellow dashed lines in **Figure 10** (O-H-N of

O12 with LYS199 and O-H-N of O20 with ARG222), which was in accordance with the binding mode proposed in thermodynamic analysis based on the rule of Ross and Subramanian.

The distances between the atoms of ASP and residues, within 5 Å, were found out and listed in **Table 5.** It showed that the distance between ASP and tryptophan (TRP214) was 3.65 nm, the value of *r* here was of no significant difference from of the value of energy transfer calculation, which in turn proved the rationality of molecular modeling results.

Note: a) Binding site of ASP on HSA (HSA is shown in cartoon. ASP is represented using spheres with hydrogen atoms omitted. The atoms of ASP are color-coded as follows: C white; O red); b) Residues adjacent to ASP; c) Residues within 5 Å (The residues of HSA are presented by lines and ASP is presented by skeleton with hydrogen atoms in b and c).

Table 5. The distance between the atoms of the ASP and the atoms of the residues (within 5 Å).

Atom of the drug	Atom of the residue	Distance
C 1	LEU219 C3	4.82
C 2	ARG218 C3	3.70
C 3	TRP214 Car	3.65
C 5	LEU238 C3	3.26
C 6	LEU219 C3	3.96
O 10	HIS242 N2	3.48
C 13	ARG257 Np13	4.52
C 4	LYS199 N4	3.81
O 9	ARG222 Np13	2.91
H 18	PHE223 Car	4.45
O 8	ALA291 C3	3.96

CONCLUSIONS

In this work, interaction of ASP with HSA was investigated *in vitro* using 3D fluorescence spectra, ultraviolet spectra, CD spectra and molecular modeling method. In order to reduce the impact of inner filter effect, all fluorescence data used in calculation was corrected. The results showed that hydrogen bonds play the major role in maintaining the only binding site with high affinity in sub-domain IIA (Sudlow's site I) of HSA molecule. The thermodynamic parameters suggested that the interaction was a spontaneous, exothermic and entropy-driven process. The distance between ASP and tryptophan residue (TRP214) was 3.71 nm, which was basically in line with molecular modeling calculation. The secondary structure changes of HSA including regular α-helix, distorted α-helix, regular β-strand, distorted β-strand, β-turns and unordered structure were calculated by CD spectra. In addition, the best score-ranked binding model recommended by molecular modeling calculation revealed a panorama of the drug-protein interaction including details of binding site, binding affinity and spatial structure at molecular level. All details were in good accordance with experiment results. In measurements of fluorescence quenching, inner-filter absorption could cause large errors in the evaluation of binding details. Therefore, this work was of great significance in understanding pharmaceutical effects of ASP.

ACKNOWLEDGEMENTS

REFERENCES

1. Howard ML, et al. Plasma protein binding in drug discovery and development. Comb Chem High Throughput Screen. 2010;13:170-187.

2. Pellegatti M, et al. Plasma protein binding and blood-free concentrations: which studies are needed to develop a drug? Expert Opin Drug Met. 2011;7;1009-1020.

3. Fanali G, et al. Human serum albumin: from bench to bedside. Mol Aspects Med. 2012;33:209-290.

4. Varshney A, et al. Ligand binding strategies of human serum albumin: how can the cargo be utilized? Chirality. 2010;22:77-87.

5. Seshasai SR, et al. Effect of aspirin on vascular and nonvascular outcomes: meta-analysis of randomized controlled trials. Arch Intern Med. 2012;172:209-216.

6. Julian D, et al. A comparison of aspirin and anticoagulation following thrombolysis for myocardial infarction (the AFTER study): a multicenter unblinded randomized clinical trial, BMJ. 1996;313:1429-1431.

7. Lewis HD, et al. Protective effects of aspirin against acute myocardial infarction and death in men with unstable angina. Results of a Veterans Administration Cooperative Study, N Engl J Med. 1983;309:396-403.

8. Alfonso L, et al. Molecular targets of aspirin and cancer prevention. Br J Cancer. 2014;111:61-67.

9. Hawkins D, et al. Structural changes in human serum albumin induced by ingestion of acetylsalicylic acid. J Clin Invest. 1969;48:536-542.

10. Alvarez HA, et al. A Molecular Dynamics Approach to Ligand-Receptor Interaction in the Aspirin-Human Serum Albumin Complex, Journal of Biophysics. 2012;7.

11. Abdollahpour N, et al. Separate and simultaneous binding effects of aspirin and amlodipine to human serum albumin based on fluorescence spectroscopic and molecular modeling characterizations: A mechanistic insight for determining usage drugs doses, J Lumin. 2011;131:1885-1899.

12. Macia, et al. (2011) A spectroscopic study of phenylbutazone and aspirin bound to serum albumin in rheumatoid diseases. Spectrochim Acta A Mol Biomol Spectrosc 82: 181-190.

13. Hosainzadeh A, et al. Probing the interaction of human serum albumin with bilirubin in the presence of aspirin by multi-spectroscopic, molecular modeling and zeta potential techniques: insight on binary and ternary systems. J Biomol Struct Dyn. 2012;29:1013-1050.

14. Dong C, et al. Studies of the interaction between demeclocycline and human serum albumin by multi-spectroscopic and molecular docking methods. Spectrochim Acta A Mol Biomol Spectrosc. 2013;103:179-186.

15. Chi Z and Liu R. Phenotypic characterization of the binding of tetracycline to human serum albumin. Bio macromolecules. 2011;12:203-209.

16. Chi Z, et al. Binding of oxytetracycline to bovine serum albumin: spectroscopic and molecular modeling investigations. J Agric Food Chem. 2010;58:10262-10269.

17. Zhang HX and Liu Y. Protein-binding properties of a designed steroidal lactam compound. Steroids. 2014;80:30-36.

18. Zhang HX and Liu E. Spectroscopic and molecular modeling investigation on the binding of a synthesized steroidal amide to protein, J Lumin. 2014;153:182-187.

19. Lakowicz JR. Principles of Fluorescence Spectroscopy (3rdedn) Springer, New York. 2006.

20. Hu YJ, et al. A Series of Novel Rare Earth Molybdotungstosilicate Heteropolyoxometalates Binding to Bovine Serum Albumin: Spectroscopic Approach, Biol Trace Elem Res. 2010;136:8-17.

21. Dehghan G, et al. Interaction of human serum albumin with Fe (III)–deferasirox studied by multispectroscopic methods, J Lumin. 2014;149:251-257.

22. Mode VA and Sisson DH. Correction of inner filter effects in fluorescence spectrometry, Anal Chem, 1974;46:200-203.

23. Seetharamappa J and Kamat BP. (Study of the interaction between fluoroquinolones and bovine serum albumin. J Pharm Biomed Anal. 2005;39:1046-1050.

24. Hu YJ, et al. Site-Selective Binding of Human Serum Albumin by Palmatine: Spectroscopic Approach, Biomacromolecules. 2010;11:106-112.

25. Naveenraj S, et al. Binding interaction between serum albumins and perylene-3,4,9,10-tetracarboxylate- A spectroscopic investigation, Dyes Pigments. 2012;94:330-337.

26. Zhang HX and Huang ZX. Biochemical evaluation of a synthesized isoflavone-selenium complex by molecular spectra, Mol Biol Rep. 2012;39:7457-7463.

27. Zhang W, et al. Comparison of interactions between human serum albumin and silver nanoparticles of different sizes using spectroscopic methods, Luminescence. 215;30:397-404.

28. Naveenraj S and Anandan. Binding of serum albumins with bioactive substances–Nanoparticles to drugs, J Photoch Photobio C. 2013;14:53-71.

29. Kandagal PB, et al. Mechanism of interaction between human serum albumin and N-alkyl phenothiazine's studied using spectroscopic methods, J Pharmaceut Biomed. 2008;47:260-267.

30. Sirotkin VA and Korolev DV. Effect of dioxane on the hydration of human serum albumin as studied by isothermal calorimetry and IR spectroscopy, Russ J Phys Chem. 2006;80:809-814.

31. Li H, et al. Caffeic acid phenethyl ester exhibiting distinctive binding interaction with human serum albumin implies the pharmacokinetic basis of propolis bioactive components, J Pharmaceut Biomed, 122 21-28.

32. Ross PD and Subramanian S. Thermodynamics of protein association reactions: forces contributing to stability. Biochemistry. 1981;20:3096-3102.

33. Suryawanshi VD, et al. A spectral deciphering the perturbation of model transporter protein (HSA) by antibacterial pyrimidine derivative: pharmacokinetic and biophysical insights, J Photochem Photobiol B. 2013;118:1-8.

34. Whitmore L and Wallace BA. Protein Secondary Structure Analyses from Circular Dichroism Spectroscopy Methods and Reference Databases, Biopolymers. 2007;89:392-400.

35. Rogers DM and Hirst JD. First-Principles Calculations of Protein Circular Dichroism in the Near Ultraviolet, Biochemistry: Us. 2004;43;11092-11102.

36. Boghaei DM, et al. Interaction of copper (II) complex of compartmental Schiff base ligand N, N'-bis (3-hydroxysalicylidene) ethylenediamine with bovine serum albumin, Spectrochim Acta A. 2007;66:650-655.

37. Gharagozlou M and Boghaei DM. Interaction of water-soluble amino acid Schiff base complexes with bovine serum albumin: Fluorescence and circular dichroism studies, Spectrochim Acta A. 2008;71;1617-1622.

38. Hegde AH, et al. Investigations to reveal the nature of interactions of human hemoglobin with curcumin using optical techniques. Int J Biol Macromol. 2013;52:133-138.

39. Forster T. Intermolecular energy migration and fluorescence, Ann Phys. 1948;437:55-75.

40. Xu ZQ, et al. Interactions between carbon Nano dots with human serum albumin and?-globulins: The effects on the transportation function, J Hazard Mater. 2016;301;242-249.

41. Mote US, et al. Fluorescence spectroscopic studies on interaction between carprofen and triton X-100 micelle, J Mol Liq. 2010;157:102-104.

42. Peng X, et al. A nonfluorescent, broad-range quencher dye for Forster resonance energy transfer assays. Anal Biochem. 2009;388:220-228.

43. He XM and Carter DC, Atomic structure and chemistry of human serum albumin, Nature. 1992;358;209-215.

44. Carter DC, et al. Three-dimensional structure of human serum albumin. Science. 1989;244:1195-1198.

45. Zhang J, et al. Interaction of Human Serum Albumin with Indomethacin: Spectroscopic and Molecular Modeling Studies, J Solution Chem. 2012;414:22-435.

46. Abou-Zied OK and Al-Lawatia N. Exploring the drug-binding site Sudlow I of human serum albumin: the role of water and Trp214 in molecular recognition and ligand binding. Chemphyschem. 2011;12:270-274.

47. Sudlow G, et al. Further characterization of specific drug binding sites on human serum albumin. Mol Pharmacol. 1976;12:1052-1061.

48. Carter DC and Ho JX. Structure of serum albumin. Adv Protein Chem. 1994;45:153-203.

49. Yan J, et al. Binding mechanism of the tyrosine-kinase inhibitor nilotinib to human serum albumin determined by 1H STD NMR, 19F NMR, and molecular modeling, J Pharmaceut Biomed 2016;124:1-9.